Copper(I) Complexes, Copper(I)/O_2 Reactivity, and Copper(II) Complex Adducts, with a Series of Tetradentate Tripyridylalkylamine Tripodal Ligands[▽]

Markus Schatz,[†] Michael Becker,[†] Florian Thaler,[†] Frank Hampel,[‡] Siegfried Schindler,*[,†] Richard R. Jacobson,[§] Zoltán Tyeklár,[§] Narashimha N. Murthy,[||,⊥] Phalguni Ghosh,[§] Qin Chen,[§] Jon Zubieta,[§,#] and Kenneth D. Karlin[§,||]

Institute of Inorganic Chemistry, University of Erlangen-Nürnberg, Egerlandstrasse 1, 91058 Erlangen, Germany, Institute of Organic Chemistry, University of Erlangen-Nürnberg, Henkestrasse 42, 91054 Erlangen, Germany, Department of Chemistry, State University of New York (SUNY) at Albany, Albany, New York 12222, and Department of Chemistry, Johns Hopkins University, Baltimore, Maryland 21218

Received August 11, 2000

Copper(I) and copper(II) complexes possessing a series of related ligands with pyridyl-containing donors have been investigated. The ligands are tris(2-pyridylmethyl)amine (tmpa), bis[(2-pyridyl)methyl]-2-(2-pyridyl)ethylamine (pmea), bis[2-(2-pyridyl)ethyl]-(2-pyridyl)methylamine (pmap), and tris[2-(2-pyridyl)ethyl]amine (tepa). The crystal structures of the protonated ligand H(tepa)ClO_4, the copper(I) complexes [Cu(pmea)]PF_6 (**1b**-PF_6), [Cu(pmap)]-PF_6 (**1c**-PF_6), and copper(II) complexes [Cu(pmea)Cl]ClO_4·H_2O (**2b**-ClO_4·H_2O), [Cu(pmap)Cl]ClO_4·H_2O (**2c**-ClO_4·H_2O), [Cu(pmap)Cl]ClO_4 (**2c**-ClO_4), and [Cu(pmea)F]$_2$(PF_6)$_2$ (**3b**-PF_6) were determined. Crystal data: H(tepa)ClO_4, formula $C_{21}H_{25}ClN_4O_4$, triclinic space group $P\bar{1}$, $Z = 2$, $a = 10.386(2)$ Å, $b = 10.723(2)$ Å, $c = 11.663(2)$ Å, $\alpha = 108.77(3)°$, $\beta = 113.81(3)°$, $\gamma = 90.39(3)°$; **1b**-PF_6, formula $C_{19}H_{20}CuF_6N_4P$, orthorhombic space group *Pbca*, $Z = 8$, $a = 14.413(3)$ Å, $b = 16.043(3)$ Å, $c = 18.288(4)$ Å, $\alpha = \beta = \gamma = 90°$; (**1c**-$PF_6$), formula $C_{20}H_{22}CuF_6N_4P$, orthorhombic space group *Pbca*, $Z = 8$, $a = 13.306(3)$ Å, $b = 16.936(3)$ Å, $c = 19.163(4)$ Å, $\alpha = \beta = \gamma = 90°$; **2b**-$ClO_4$·$H_2O$, formula $C_{19}H_{22}Cl_2CuN_4O_5$, triclinic space group $P\bar{1}$, $Z = 4$, $a = 11.967(2)$ Å, $b = 12.445(3)$ Å, $c = 15.668(3)$ Å, $\alpha = 84.65(3)°$, $\beta = 68.57(3)°$, $\gamma = 87.33(3)°$; **2c**-ClO_4·H_2O, formula $C_{20}H_{24}Cl_2CuN_4O_5$, monoclinic space group $P2_1/c$, $Z = 4$, $a = 11.2927(5)$ Å, $b = 13.2389(4)$ Å, $c = 15.0939(8)$ Å, $\alpha = \gamma = 90°$, $\beta = 97.397(2)°$; **2c**-ClO_4, formula $C_{20}H_{22}Cl_2CuN_4O_4$, monoclinic space group $P2_1/c$, $Z = 4$, $a = 8.7682(4)$ Å, $b = 18.4968(10)$ Å, $c = 13.2575(8)$ Å, $\alpha = \gamma = 90°$, $\beta = 94.219(4)°$; **3b**-PF_6, formula [$C_{19}H_{20}CuF_7N_4P$]$_2$, monoclinic space group $P2_1/n$, $Z = 2$, $a = 11.620(5)$ Å, $b = 12.752(5)$ Å, $c = 15.424(6)$ Å, $\alpha = \gamma = 90°$, $\beta = 109.56(3)°$. The oxidation of the copper(I) complexes with dioxygen was studied. [Cu(tmpa)(CH_3CN)]$^+$ (**1a**) reacts with dioxygen to form a dinuclear peroxo complex that is stable at low temperatures. In contrast, only a very labile peroxo complex was observed spectroscopically when **1b** was reacted with dioxygen at low temperatures using stopped-flow kinetic techniques. No dioxygen adduct was detected spectroscopically during the oxidation of **1c**, and **1d** was found to be unreactive toward dioxygen. Reaction of dioxygen with **1a**-PF_6, **1b**-PF_6, and **1c**-PF_6 at ambient temperatures leads to fluoride-bridged dinuclear copper(II) complexes as products. All copper(II) complexes were characterized by UV−vis, EPR, and electrochemical measurements. The results manifest the dramatic effects of ligand variations and particularly chelate ring size on structure and reactivity.

Introduction

Copper ions are found in the active sites of a large number of metalloproteins involved in important biological electron-transfer reactions, as well as in redox processing of molecular oxygen.[1−7] The former comprises "blue" ("type 1") copper sites in electron-transfer proteins or multicopper oxidases,[1,8−10] while the latter includes hemocyanins (arthropodal and molluscan blood O_2-carrier proteins),[11−13] oxygenases inserting O atoms

[▽] Dedicated to Professor Dr. Ernst G. Jäger on the occasion of his 65th birthday.

* To whom correspondence should be addressed. Fax: 49-(0)9131-8527387. E-mail: schindls@anorganik.chemie.uni-erlangen.de.

[†] Institute of Inorganic Chemistry, University of Erlangen-Nürnberg.

[‡] Institute of Organic Chemistry, University of Erlangen-Nürnberg.

[§] Department of Chemistry, State University of New York (SUNY) at Albany.

[||] Department of Chemistry, Johns Hopkins University.

[⊥] Current address: Department of Chemistry, IIT Madras 600036, India.

[#] Current address: Department of Chemistry, Syracuse University, Syracuse, NY 13244.

(1) Holm, R. H.; Kennepohl, P.; Solomon, E. I. *Chem. Rev.* **1996**, *96*, 2239−2314.

(2) Karlin, K. D.; Zuberbühler, A. D. In *Bioinorganic Catalysis*, 2nd ed.; Reedijk, J., Bouwman, E., Eds.; Marcel Dekker: New York, 1999; pp 469−534.

(3) Fox, S.; Karlin, K. D. In *Active Oxygen in Biochemistry*; Valentine, J. S., Foote, C. S., Greenberg, A., Liebman, J. F., Eds.; Blackie Academic and Professional: Glasgow, Scotland, 1995; pp 188−231.

(4) Kaim, W.; Rall, J. *Angew. Chem.* **1996**, *108*, 47−64.

(5) Kitajima, N.; Moro-oka, Y. *Chem. Rev.* **1994**, *94*, 737−757.

(6) Kitajima, N. *Adv. Inorg. Chem.* **1992**, *39*, 1−77.

(7) Karlin, K. D., Tyeklár, Z., Eds. *Bioinorganic Chemistry of Copper*; Chapman & Hall: New York, 1993.

(8) Messerschmidt, A. *Inorg. Chem.* **1993**, *32*, 121−185.

(9) Adman, E. T. *Adv. Protein Chem.* **1991**, *42*, 145−197.

(10) Chapman, S. K. *Perspect. Bioinorg. Chem.* **1991**, *1*, 95−140.

(11) Solomon, E. I.; Sundaram, U. M.; Machonkin, T. E. *Chem. Rev.* **1996**, *96*, 2563−2605.

(12) Magnus, K. A.; Ton-That, H.; Carpenter, J. E. *Chem. Rev.* **1994**, *94*, 727−735.

10.1021/ic000924n CCC: $20.00
Published on Web 04/07/2001

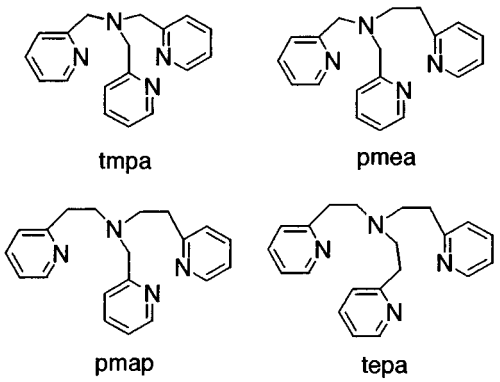

$[Cu(tmpa)(MeCN)]^+$ (**1a**), $[Cu(pmea)]^+$ (**1b**),
$[Cu(pmap)]^+$ (**1c**), $[Cu(tepa)]^+$ (**1d**),
$[Cu(tmpa)Cl]^+$ (**2a**), $[Cu(pmea)Cl]^+$ (**2b**),
$[Cu(pmap)Cl]^+$ (**2c**), $[Cu(tepa)Cl]^+$ (**2d**),
$[Cu(tmpa)F]_2^{2+}$ (**3a**), $[Cu(pmea)F]_2^{2+}$ (**3b**),
$[Cu(pmap)F]_2^{2+}$ (**3c**), $[Cu(tepa)F]_2^{2+}$ (**3d**),

Figure 1. Tripodal ligands tmpa, pmea, pmap, and tepa and abbrevations used for copper complexes.

into substrates,[11,14] and oxidases coupling substrate oxidations to copper-mediated dioxygen reduction to hydrogen peroxide or water.[8,11,15]

Protein active-site chemistry is governed by the close environment about the metal ion provided by the protein amino acids (i.e., the first and/or second metal coordination shell).[16,17] It is therefore of interest to employ model compound investigations[2−7,18−22] to understand how a ligand environment (as determined by the identity of its donor atoms and their arrangement) modulates details of structure, Cu(II)/Cu(I) redox properties, Cu(I)/O_2 reactivity, and Cu(I) or Cu(II) spectroscopic properties. In this report we describe aspects of the copper(I) and copper(II) chemistry of a family of pyridylalkylamine tripodal tetradentate ligands, the "parent" ligand being tmpa (tris-[(2-pyridyl)methyl]amine) (Figure 1). $[Cu(tmpa)(CH_3CN)]^+$ (**1a**) has proven to be an important compound in dioxygen reactivity studies,[2] forming a *trans*-μ-1,2-peroxo-dicopper(II) product $[\{Cu(tmpa)\}_2(O_2)]^{2+}$, which has been characterized in detail, including by X-ray crystallography,[23,24] and for its electronic structure.[25] The kinetics and thermodynamics of the $[Cu(tmpa)(CH_3CN)]^+$ reaction with O_2 in EtCN and acetone solvents have been elucidated[26,27] and compared in detail to a family of close analogue ligand (L_Q) complexes that are varied sterically and/or electronically with quinolyl groups systematically replacing each pyridyl group in tmpa.[26,28] Systematic quinolyl-for-pyridyl substitution dramatically influences the redox properties of $[(L_Q)Cu^I]^+$ complexes,[29] and the kinetics and thermodynamics of O_2 reaction compared to that of **1a**, including whether a superoxo intermediate, $[(CuL)(O_2)]^+$, is observed.[26,28]

In its copper(II) chemistry, tmpa forms pentacoordinate species $[Cu^{II}(tmpa)(X)]^{n+}$ (X = anion or neutral ligand),[30] including $[Cu^{II}(tmpa)(Cl)]^+$ (**2a**), a trigonal bipyramidal Cu(II) complex.[31] In fact, the structure, redox potential, and UV−vis and EPR properties of **2a** contrast with those of the quinolyl-substituted complex analogues $[Cu^{II}(L_Q)(Cl)]^+$, the latter being distorted toward a square-based pyramidal structure and having more positive (i.e., favoring Cu(I)) redox potentials.[32] The same is true in comparing $[Cu^{II}(tmpa)(Cl)]^+$ (**2a**) with $[Cu^{II}(tepa)(Cl)]^+$ (**2d**); the longer-armed tepa ligand (Figure 1) leads to a complex **2d** that is nearly perfectly square-based pyramidal in structure, possessing corresponding EPR and UV−vis properties and having a redox potential nearly 0.5 V more positive.[31]

Clearly, all of these kinds of studies with either Cu(I) or Cu(II) with similar ligands show that small changes in ligand architecture can strongly influence the chemistry.[33] In enzyme-active sites, the nature and juxtaposition of ligand donors are highly evolved to allow or to force the metal ion chemistry to carry out the desired function. Thus, further studies of ligand influences, as made possible when employing systematically varied systems, can provide valuable insights into fundamental aspects of biologically relevant coordination chemistry. It is against this background that we further study and compare/contrast the copper(I), Cu(I)/O_2 reactivity, and Cu(II) complexes of the ligands shown in Figure 1. In particular, the chemistry of the ligands pmap and pmea is emphasized, with chelate ring size properties being intermediate in comparison with their previously more studied analogues tmpa and tepa.

Experimental Section

Materials and Methods. Reagents and solvents used were of commercially available reagent quality. Acetonitrile, propionitrile, diethyl ether, and acetone used in the syntheses of the copper(I) complexes or in the kinetic studies were dried in the usual way. $[Cu(CH_3CN)_4]ClO_4$, $[Cu(CH_3CN)_4]PF_6$, and tmpa were synthesized according to the literature.[24,34,35] All column chromatography of ligands was carried out by "flash chromatography" using alumina (80−200 mesh, MCB).[36] Purity of the ligands was judged by TLC and ^{1}H NMR. $[Cu(tmpa)(CH_3CN)]PF_6$ (**1a**-PF_6), $[Cu(tmpa)(CH_3CN)]ClO_4$ (**1a**-ClO_4), $[Cu(tmpa)Cl]ClO_4$ (**2a**-ClO_4), $[Cu(tepa)]PF_6$ (**1d**-PF_6), and $[Cu(tepa)Cl]PF_6$ (**2d**-PF_6) were prepared as described earlier.[24,31,37]

(13) Cuff, M. E.; Miller, K. I.; van Holde, K. E.; Hendrickson, W. A. *J. Mol. Biol.* **1998**, *278*, 855−870.
(14) Decker, H.; Dillinger, R.; Tuczek, F. *Angew. Chem., Int. Ed.* **2000**, *39*, 1591−1595.
(15) Klinman, J. P. *Chem. Rev.* **1996**, *96*, 2541−2561.
(16) Karlin, S.; Zhu, Z.-Y.; Karlin, K. D. *Proc. Natl. Acad. Sci. U.S.A.* **1997**, *94*, 14225−14230.
(17) Karlin, K. D.; Zhu, Z.-Y.; Karlin, S. *J. Biol. Inorg. Chem.* **1998**, *3*, 172−187.
(18) Spodine, E.; Manzur, J. *Coord. Chem. Rev.* **1992**, *119*, 171−198.
(19) Liang, H.-C.; Dahan, M.; Karlin, K. D. *Curr. Opin. Chem. Biol.* **1999**, *3* (2), 168−175.
(20) Karlin, K. D. *Science* **1993**, *261*, 701−708.
(21) Schindler, S. *Eur. J. Inorg. Chem.* **2000**, 2311−2326.
(22) Blackman, A. G.; Tolman, W. B. In *Structure and Bonding: Metal-Oxo and Metal-Peroxo Species in Catalytic Oxidations*; Meunier, B., Ed.; Springer, Berlin, 2000; Vol. 97, pp 179−211.
(23) Jacobson, R. R.; Tyeklár, Z.; Farooq, A.; Karlin, K. D.; Liu, S.; Zubieta, J. *J. Am. Chem. Soc.* **1988**, *110*, 3690−3692.
(24) Tyeklár, Z.; Jakobson, R. R.; Wei, N.; Murthy, N. N.; Zubieta, J.; Karlin, K. D. *J. Am. Chem. Soc.* **1993**, *115*, 2677−2689.
(25) Baldwin, M. J.; Ross, P. K.; Pate, J. E.; Tyeklar, Z.; Karlin, K. D.; Solomon, E. I. *J. Am. Chem. Soc.* **1991**, *113*, 8671−8679.
(26) Karlin, K. D.; Wei, N.; Jung, B.; Kaderli, S.; Niklaus, P.; Zuberbühler, A. D. *J. Am. Chem. Soc.* **1993**, *115*, 9506−9514.
(27) Karlin, K. D.; Lee, D.-H.; Kaderli, S.; Zuberbühler, A. D. *Chem. Commun.* **1997**, 475.
(28) Karlin, K. D.; Kaderli, S.; Zuberbühler, A. D. *Acc. Chem. Res.* **1997**, *30*, 139−147.
(29) Wei, N.; Murthy, N. N.; Chen, Q.; Zubieta, J.; Karlin, K. D. *Inorg. Chem.* **1994**, *33*, 1953−1965.
(30) Zubieta, J.; Karlin, K. D.; Hayes, J. C. In *Copper Coordination Chemistry: Biochemical and Inorganic Perspectives*; Karlin, K. D., Zubieta, J., Eds.; Adenine Press: Albany, NY, 1983; pp 97−108.
(31) Karlin, K. D.; Hayes, J. C.; Juen, S.; Hutchinson, J. P.; Zubieta, J. *Inorg. Chem.* **1982**, *21*, 4106−4108.
(32) Wei, N.; Murthy, N. N.; Karlin, K. D. *Inorg. Chem.* **1994**, *33*, 6093−6100.
(33) Obias, H. V.; van Strijdonck, G. P. F.; Lee, D.-H.; Ralle, M.; Blackburn, N. J.; Karlin, K. D. *J. Am. Chem. Soc.* **1998**, *120*, 9696−9697.
(34) Hemmerich, P.; Sigwart, C. *Experientia* **1963**, *XIX*, 488−489.

Preparation and handling of air-sensitive compounds were carried out in a glovebox filled with argon (either in a Vacuum Atmospheres drybox or a Braun glovebox; water and dioxygen less than 1 ppm) or using standard Schlenk techniques. Deoxygenation of solvents and solutions was effected by either repeated vacuum/purge cycles or thorough bubbling (20 min) with argon. Solid samples were stored and transferred, and samples for IR and NMR spectra were prepared in the glovebox.

UV−vis spectra were measured on a Hewlett-Packard 8452 A or a Shimadzu UV-160 spectrophotometer using standard 1 cm quartz cuvettes. ^{1}H and ^{13}C NMR spectra were recorded on a Varian XL-300 or a Bruker DXP 300 AVANCE spectrometer. Infrared spectra were recorded as either Nujol mulls or KBr pellets on a Perkin-Elmer 283 or 710B instrument and calibrated with polystyrene (1601.8 cm^{-1}). Electron paramagnetic resonance (EPR) spectra were obtained from frozen solutions (77 K) and powder samples (room temperature) using 4 mm OD quartz tubes in a Varian model E-4 spectrometer operating at X-band. The field was calibrated with a powder sample of diphenylpicrylhydrazyl (DPPH, $g = 2.0037$). Solvents used were CH_3CN, CH_2Cl_2/toluene (4:1, v/v), or H_2O/MeOH/EtOH (1:4:15, v/v) with concentrations of the copper complexes at approximately 10^{-3} M. Room-temperature magnetic moments were determined with a Johnson Mathey magnetometer that was calibrated by using $Hg[Co(SCN)_4]$.

Cyclic voltammetry was carried out using a Bioanalytical Systems (BAS) CV-27 voltammograph and Houston Instruments model 100 *XY* recorder. The measurements were performed at 25 °C in DMF solutions containing 0.2 M n-Bu_4NPF_6 and 10^{-3}−10^{-4} M copper(II) complex deoxygenated by bubbling with nitrogen. The experiments utilized a three-chambered electrochemical cell in which the working solution compartment was separated from the other two by fine glass frits. The reference electrode for the electrochemical measurements was an Ag/AgCl electrode (BAS MF-1052), which was determined to be 0.15 V positive of NHE. The working and auxiliary electrodes were a glassy carbon disk and coiled platinum wire, respectively.

Electrical conductivity measurements were carried out in CH_3CN with a Barnstead model PM-70CB conductivity bridge and YSI model 3403 conductivity cell. The cell constant was determined with a standard aqueous solution of KCl (0.100 M). The molar conductivity, Λ_m, of a sample solution was determined from $\Lambda_m = 1000K/c_m$ where K is the cell constant divided by the measured resistance and c_m is the molar concentration of the solute (ca. 1×10^{-3} M).

Elemental analyses were carried out at the University of Erlangen−Nürnberg or performed by Desert Analytics (formerly MicAnal), Tucson, AZ, or Galbraith Laboratories, Inc., Knoxville, TN.

Variable-Temperature Stopped-Flow Measurements. Solutions of complexes for the collection of time-resolved UV−vis spectra were prepared in the glovebox and transferred with syringes to the low-temperature stopped-flow instrument. A dioxygen saturated solution was prepared by bubbling dioxygen through propionitrile or acetone in a syringe (solubility of dioxygen at 25 °C in propionitrile is 0.0088 M,[26] and in acetone it is 0.0102 M[38]). Dilution was accomplished by mixing the solution with argon-saturated propionitrile or acetone. The reaction was studied under pseudo-first-order conditions ([complex] $\ll$ [O_2]), and time-resolved UV−vis spectra of the reactions of dioxygen with copper(I) complexes were recorded with a modified Hi-Tech SF-3L low-temperature stopped-flow unit (Salisbury, U.K.) equipped with a J&M TIDAS 16-500 photodiode array spectrophotometer (J&M, Aalen, Germany). Data treatment was carried out using the integrated J&M software Kinspec or the program Specfit (Spectrum Software Associates, Chapel Hill, NC).

X-ray Structure Determination of H(tepa)ClO_4, 1c-PF_6, 2b-ClO_4·H_2O, 2c-ClO_4·H_2O, and 2c-ClO_4. Single crystals were coated with polyfluorether oil and mounted on a glass fiber. Lorentz, polarization, and empirical absorption corrections were applied. Space groups were determined from systematic absences and subsequent least-squares refinement. The structure was solved by direct methods. The parameters were refined using SHELXL-93[39,40] and SHELXL-97.[41] Non-hydrogen atoms were refined with anisotropic thermal parameters. The hydrogen atoms were fixed in idealized positions using a riding model. In H(tepa)-ClO_4 the hydrogen H1 at N1 could be localized and was free isotropic refined. Scattering factors were taken from the literature.[42]

X-ray Structure Determination of 1b-PF_6 and 3b-PF_6. Epoxy-covered crystals of both complexes were mounted on glass fibers. Centering and least-squares routines were carried out on 25 reflections to obtain the unit cell parameters and Bravais lattice type. The structure was solved by the Patterson method. All atoms, with the exception of hydrogen and carbon, were refined anisotropically. Hydrogen atoms were included in the final stages of refinement with carbon−hydrogen bond lengths set at 0.96 Å. For **3b**-PF_6, the pyridyl rings were refined as rigid hexagons (d(C−C(N)) = 1.395 Å) because of the limited number of data. Full details of the crystallographic methodologies may be found in the given reference.[43]

Syntheses of Ligands and Complexes. *Caution! Perchlorate salts are potentially explosive and should be handled with great care.*

1. Bis[(2-pyridyl)methyl]-2-(2-pyridyl)ethylamine (pmea). Pmea was synthesized similar to published procedures.[44,45] To a suspension of 24.6 g (177 mmol) of anhydrous potassium carbonate in 150 mL of MeOH was added 6.12 g (50.1 mmol) of 2-(2-aminoethyl)pyridine and 18.1 g (110 mmol) of 2-picolyl chloride hydrochloride. The reagents were stirred while being heated at reflux under nitrogen for 5 days. The dark-brown reaction mixture was cooled and filtered to remove potassium carbonate, and the MeOH was removed. The product was then washed with 150 mL of 15% NaOH and extracted with dichloromethane (4 × 50 mL), and the extracts were dried over $MgSO_4$. Removal of the solvent gave a crude oil that was chromatographed on alumina with a 98/2 (v/v) mixture of ethyl acetate/MeOH ($R_f = 0.44$). The purified ligand was obtained as a dark-orange oil in 44% yield (6.64 g). ^{1}H NMR (CD_3CN): δ 8.44 (m, 3 H), 7.60 (m, 3 H), 7.34 (m, 3 H), 7.14 (m, 3 H), 3.82 (s, 4 H), 2.93 (m, 4 H). ^{13}C NMR (CD_3CN): δ 161.48 (2′-py), 160.78 (2-py), 149.88 (6′-py), 149.62 (6-py), 137.09 (4-py), 136.93 (4′-py), 124.16 (3′-py), 123.57 (3-py), 122.79 (5-py), 121.97 (5′-py), 60.84 (1″-CH_2), 54.92 (2″-CH_2), 36.49 (3″-CH_2).

2. Bis[2-(2-pyridyl)ethyl]-(2-pyridyl)methylamine (pmap). Pmap was synthesized similar to a procedure recently described.[46] A mixture of 2-(aminomethyl)pyridine (20.0 g, 185 mmol), 2-vinylpyridine (77.3 g, 735 mmol), glacial acetic acid (30 mL), and 250 mL of MeOH was refluxed gently for 6 days. The resulting brown mixture was cooled and the MeOH removed by rotary evaporation. The resulting oil was stirred with 200 mL of 15% NaOH and extracted with dichloromethane (4 × 50 mL). The organic phase was dried with $MgSO_4$ and filtered through a coarse frit, and the solvent was removed. Excess 2-vinylpyridine was removed by warming the product gently (45 °C) under vacuum overnight. The ligand was purified by column chromatography on alumina using a mixture of ethyl acetate and methanol (98/2, v/v) as eluent ($R_f = 0.49$). The purified product was obtained as a viscous brown oil in 76% yield (44.5 g). ^{1}H NMR (CD_3CN): δ 8.45 (m, 3 H), 7.54 (m, 3 H), 7.08 (m, 6 H), 3.82 (s, 2 H), 2.91 (m, 8 H). ^{13}C NMR

(35) Kubas, G. J.; Monzyk, B.; Crumbliss, A. L. *Inorg. Synth.* **1979**, *19*, 90.
(36) Still, W. C.; Kahn, M.; Mitra, A. *J. Org. Chem.* **1978**, *43*, 2923−2925.
(37) Karlin, K. D.; Hayes, J. C.; Hutchinson, J. P.; Hyde, J. R.; Zubieta, J. *Inorg. Chim. Acta* **1982**, *64*, L219-L220.
(38) Lühring, P.; Schumpe, A. *J. Chem. Eng. Data* **1989**, *34*, 250−252.
(39) Sheldrick, G. M. *SHELX-93, Program for refinement of crystal structures*; University of Göttingen: Göttingen, Germany, 1993.
(40) Sheldrick, G. M. SHELXL-93. In *Crystallographic Computing 3*; Sheldrick, G. M., Krüger, C., Goddard, R., Eds.; Oxford University, 1993; pp 175−189.
(41) Sheldrick, G. M. *SHELX-97, Program for refinement of crystal structures*; University of Göttingen: Göttingen, Germany, 1997.
(42) Cromer, D. T.; Waber, J. T. In *International Tables for X-ray Crystallography*; Ibers, J. A., Hamilton, W. C., Eds.; Kynoch: Birmingham, England, 1974.
(43) Sheldrick, G. M. *Nicolet SHELXTL*; Nicolet XRD Corp.: Cupertino, CA, 1979.
(44) Hojland, F.; Toftlund, H.; Yde-Andersen, S. *Acta Chem. Scand.* **1983**, *37*, 251−257.
(45) Oki, A. R.; Glerup, J.; Hodgson, D. J. *Inorg. Chem.* **1990**, *29*, 2435−2441.
(46) Dietrich, J.; Heinemann, F. W.; Schrodt, A.; Schindler, S. *Inorg. Chim. Acta* **1999**, *288*, 206−209.

(CD_3CN): δ 161.51 (2′-py), 161.16 (2-py), 149.86 (6′-py), 149.41 (6-py), 136.88 (4-py), 136.82 (4′-py), 124.10 (3′-py), 123.40 (3-py), 122.55 (5-py), 121.86 (5′-py), 60.84 (1″-CH_2), 54.68 (2″-CH_2), 36.49 (3″-CH_3).

3. Tris[2-(2-pyridyl)ethyl]amine (tepa). A mixture of ammonium chloride (69.4 g, 1.30 mol) and 2-vinylpyridine (72.4 g, 689 mmol) in 190 mL of water and 30 mL of methanol was refluxed for 42 h. The resulting red-brown mixture was cooled and stirred with 200 mL of 15% NaOH and then extracted with dichloromethane (4 × 50 mL) to remove the product from the aqueous phase. The organic phase was dried over $MgSO_4$ and filtered through a coarse frit. The solvent was removed by rotary evaporation, leaving a brown oil that was chromatographed on alumina using a 98/2 (v/v) mixture of ethyl acetate/methanol as eluent ($R_f = 0.57$). The purified product was obtained as a slightly viscous yellow oil in 23% yield (17.8 g). ^{1}H NMR (CD_3CN): δ 8.47 (m, 3 H), 7.53 (m, 3 H), 7.06 (m, 6 H), 2.91 (m, 6 H), 2.82 (m, 6 H). ^{13}C NMR (CD_3CN): δ 161.68 (2′-py), 149.90 (6′-py), 136.87 (4′-py), 124.13 (3′-py), 121.86 (5′-py), 54.45 (2″-CH_2), 36.54 (3″-CH_2).

4. [Cu(pmea)]PF_6 (1b-PF_6). A solution of pmea (1.01 g, 3.32 mmol) in 20 mL of CH_3CN was added dropwise, with stirring, to 1.24 g (3.33 mmol) of [$Cu(CH_3CN)_4$]PF_6 under argon. The resulting yellow-brown solution was stirred for $^1/_2$ h, at which time enough dry diethyl ether was added to cause a slight cloudiness (ca. 50 mL). The solution was filtered through a medium-porosity frit and the complex precipitated by further addition of ether (200 mL). The ether was added slowly with vigorous stirring to overcome the tendency of the complex to oil out. The supernatant was removed and the solid washed with 75 mL of additional ether. Drying in vacuo yielded 1.22 g (72%) of a deep-yellow powder. Slow diffusion of diethyl ether into acetonitrile solution of compounds **1b**-PF_6 yielded yellow crystals that were suitable for X-ray crystallographic analysis. Anal. Calcd for $C_{19}H_{20}CuF_6N_4P$: C, 44.49; H, 3.93; N, 10.92. Found: C, 45.01; H, 4.10; N, 11.09. ^{1}H NMR (CD_3CN): δ 8.75 (br, 3 H), 7.78 (m, br, 3 H), 7.36 (m, br, 6 H), 4.03 (br, 4 H), 3.05 (br, 2 H), 2.94 (br, 2 H). ^{13}C NMR (CD_3CN): δ 160.16 (2′-py), 157.89 (br, 2-py), 150.24 (6′-py), 149.62 (br, 6-py), 138.45 (4-py), 138.21 (4′-py), 126.55 (3′-py), 125.24 (br, 3-py), 124.88 (br, 5-py), 123.88 (5′-py), 60.09 (br, 1"-CH_2), 55.21 (br, 2"-CH_2), 36.72 (3"-CH_2). IR (Nujol; cm^{-1}): ca. 2900 (vs, C−H), 1600 (s, C═C), 1565 (m), 1440 (vs), 1375 (s), 1310 (s), 1300 (s), 1270 (s), 1215 (w), 1150 (s), 1120 (s), 1090 (m), 1050 (s), 1030 (m), 1005 (w), 970 (m), 940 (w), 915 (w), ca. 840 (vs, br, PF_6^-), 780 (vs), 720 (s), 660 (w), 640 (w), 630 (w).

5. [Cu(pmap)]PF_6 (1c-PF_6). The ligand pmap (2.01 g, 6.31 mmol) was dissolved in 35 mL of CH_3CN and added dropwise to 2.34 g (6.28 mmol) of [$Cu(CH_3CN)_4$]PF_6 while being stirred under argon for 20 min. To the resulting yellow-brown solution was added diethyl ether until the complex began to precipitate (ca. 75 mL). The solution was then filtered through a medium-porosity frit and the complex precipitated by addition of 150 mL of ether. The supernatant was decanted, and the complex was washed with 100 mL of additional Et_2O. The solid was dried in vacuo to yield 2.84 g (86%) of a bright-yellow microcrystalline powder. Slow diffusion of diethyl ether into acetonitrile solution of compound **1c**-PF_6 yielded yellow crystals that were suitable for X-ray crystallographic analysis. Anal. Calcd for $C_{20}H_{22}CuF_6N_4P$: C, 45.59; H, 4.21; N,10.63. Found: C, 45.87; H, 4.22; N, 10.50. ^{1}H NMR (CD_3CN): δ 8.76 (m, 3 H), 7.76 (m, 3 H), 7.31 (m, 6 H), 4.03 (s, 2 H), 3.02 (br, 4 H), 2.83 (br, 4 H). ^{13}C NMR (CD_3CN): δ 160.61 (2′-py), 158.22 (2-py), 150.46 (6′-py), 149.08 (6-py), 138.36 (4′-py), 138.01 (4-py), 126.44 (3′-py), 125.07 (3-py), 124.29 (5-py), 123.84 (5′-py), 60.74 (1″-CH_2). 55.21 (2″-CH_2), 35.42 (3″-CH_2). IR (Nujol; cm^{-1}): ca. 2920 (vs, C−H), 2850 (vs), 1600 (s, C═C), 1565 (m), 1450 (vs), 1380 (vs), 1320 (vs), 1265 (m), 1245 (w), 1230 (w), 1210 (w), 1155 (m), 1120 (s), 1055 (m), 1030 (m), 990 (w), 960 (w), 950 (w), 935 (w), 900 (s), 875 (s), ca. 835 (vs, br, PF_6^-), 785 (s), 775 (s), 760 (vs), 750 (vs), 720 (s), 550 (vs).

6. [Cu(pmea)Cl]PF_6 (2b-PF_6). Pmea (0.506 g, 1.66 mmol) and $CuCl_2 \cdot 2H_2O$ (0.283 g, 1.66 mmol) were added to 40 mL of MeOH and allowed to stir for 30 min. To the resulting blue-green solution was added a solution of $NaPF_6$ (1.38 g, 8.22 mmol) in 20 mL of MeOH. A crude precipitate was obtained by addition of 200 mL of diethyl ether and storage at 8 °C overnight. Following removal of the solvent, the precipitate was redissolved in CH_2Cl_2 (50 mL) and filtered and the solution layered with ether. Storage of the mixture at 8 °C for 2 days resulted in the formation of a semicrystalline blue solid. Recrystallization of this material from CH_2Cl_2/Et_2O afforded analytically pure **2b**-PF_6 as a fine blue powder (0.611 g, 68%). IR (Nujol; cm^{-1}): ca. 2900 (vs, C−H), 1605 (s, C═C), 1575 (m), 1450 (vs), 1430 (s), 1380 (vs), 1360 (m), 1340 (m), 1310 (s), 1290 (s), 1255 (m), 1230 (w), 1210 (w), 1160 (s), 1110 (m), 1090 (w), 1060 (s),1045 (m), 1030 (s), 1000 (s), 980 (w), 960 (m), 945 (m), 900 (s), ca. 835 (vs, br, PF_6^-), 780 (vs), 760 (vs), 740 (s), 720 (s), 655 (m), 635 (m), 560 (vs). UV−vis (CH_3CN; λ_{max}, nm (ϵ, M^{-1} cm^{-1})): 256 (13700), 283 (sh, 3260), 666 (150). Molar conductivity: 158 Ω^{-1} cm^2 mol^{-1}. EPR (CH_2Cl_2/toluene): $g_{\|} = 2.224$, $A_{\|} = 168 \times 10^{-4}$ cm^{-1}. Magnetism (solid state, room temperature): $\mu_{eff} = 1.95 \pm 0.05$ μ_B/Cu.

7. [Cu(pmea)Cl]$ClO_4 \cdot H_2O$ (2b-$ClO_4 \cdot H_2O$). To a solution of pmea (0.76 g, 2.5 mmol) in 10 mL of methanol a solution of $Cu(ClO_4)_2 \cdot 6H_2O$ (0.46 g, 1.25 mmol) and $CuCl_2 \cdot 2H_2O$ (0.21 g, 1.25 mmol) in 20 mL of water was added. It was stirred for a few minutes and then filtered. Crystals suitable for X-ray analysis formed soon afterward (0.65 g, 50%). Anal. Calcd for $C_{19}H_{20}Cl_2CuN_4O_4 \cdot H_2O$: C, 43.81; H, 4.26; N, 10.76. Found: C, 44.10; H, 4.09; N, 10.62.

8. [Cu(pmap)Cl]$PF_6 \cdot {}^1/_4CH_2Cl_2$ (2c-$PF_6 \cdot {}^1/_4CH_2Cl_2$). Pmap (0.514 g, 1.61 mmol) and $CuCl_2 \cdot 2H_2O$ (0.274 g, 1.61 mmol) were dissolved in a total of 40 mL of MeOH and allowed to stir for 30 min. To the resulting blue-green solution was added 1.32 g (7.86 mmol) of $NaPF_6$ in 20 mL of MeOH whereupon a blue precipitate was immediately formed. The mixture was cooled to 8 °C for 4 h to ensure complete precipitation, and the supernatant was decanted. The solid was redissolved in CH_2Cl_2 (75 mL) and filtered, and the solution was layered with diethyl ether (175 mL). Deep-blue crystals were obtained from this preparation after refrigeration for 48 h. A final recrystallization from CH_2Cl_2/Et_2O gave 0.723 g (77%) of analytically pure material. Anal. Calcd for $C_{20.25}H_{22.5}Cl_{1.5}CuF_6N_4P$: C, 41.68; H, 3.89; N, 9.60. Found: C, 41.70; H, 4.09; N, 9.36. IR (Nujol; cm^{-1}): ca. 2900 (vs, CH), 1605 (s, C═C), 1570 (m), 1485 (s), 1455 (vs), 1380 (s), 1360 (m), 1320 (s), 1305 (s), 1285 (w), 1270 (m), 1230 (w), 1215 (w), 1195 (w), 1160 (s), 1110 (m), 1060 (m), 1030 (s), 1020 (m), 1005 (m), 990 (w), 960 (m), 950 (m), 880 (s), ca. 840 (vs, br, PF_6^-), 775 (vs), 765 (vs), 740 (s), 730 (s), 705 (w), 650 (m), 640 (m), 590 (s), 560 (vs). UV−vis (CH_3CN; λ_{max}, nm (ϵ, M^{-1} cm^{-1})): 257 (13900), 285 (sh, 3820), 639 (192), 898 (sh, 22.5). Molar conductivity: $\Lambda_m = 153$ Ω^{-1} cm^2 mol^{-1}. EPR (CH_2Cl_2/toluene): $g_{\|} = 2.217$, $A_{\|} = 166 \times 10^{-4}$ cm^{-1}. Magnetism (solid state, room temperature): $\mu_{eff} = 1.93 \pm 0.05$ μ_B/Cu.

9. [Cu(pmap)Cl]$ClO_4 \cdot 0.5H_2O$ (2c-$ClO_4 \cdot 0.5H_2O$). To a solution of pmap (0.796 g, 2.5 mmol) in 10 mL of methanol a solution of $Cu(ClO_4)_2 \cdot 6H_2O$ (0.46 g, 1.25 mmol) and $CuCl_2 \cdot 2H_2O$ (0.21 g, 1.25 mmol) in 20 mL of water was added. It was stirred for a few minutes and then filtered. Crystals suitable for X-ray analysis formed soon afterward (0.98 g, 75%). Anal. Calcd for $C_{20}H_{22}Cl_2CuN_4O_4 \cdot 0.5H_2O$: C, 45.68; H, 4.41; N, 10.65. Found: C, 45.83; H, 4.52; N, 10.63.

10. [Cu(pmea)F]$_2$(PF_6)$_2$ (3b-PF_6). A solution of **1b**-PF_6 (1.69 g, 3.29 mmol) in 40 mL of Ar-saturated CH_3CN was oxygenated by bubbling with O_2 gas for 15 min. The solution, which had become a cloudy blue-green color, was filtered and the solvent removed by rotary evaporation. The residue was dissolved in 100 mL of a 3:1 mixture of CH_2Cl_2/CH_3CN, and the solution was layered with diethyl ether (150 mL). Storage of the mixture at 8 °C resulted in the formation of a quantity of dark-blue crystals and a substantial amount of green precipitate. The solvent was decanted, and the crystalline material was redissolved in CH_2Cl_2 (150 mL) with vigorous stirring. The solution was layered with ether (100 mL) and stored at 8 °C for several days to again give a crystalline solid and a small quantity of precipitate. A final recrystallization from CH_2Cl_2 yielded 0.747 g (43% based on Cu) of analytically pure **3b**-PF_6. Anal. Calcd for $C_{38}H_{40}Cu_2F_{14}P_2$: C, 42.90; H, 3.79; N, 10.53; F, 25.00. Found: C, 43.00; H, 3.87; N, 10.66; F 24.76. IR (Nujol; cm^{-1}): ca. 2900 (vs, C−H), 1650 (w), 1600 (s, C═C), 1570 (m), 1450 (vs), 1425 (s), 1375 (s), 1350 (m), 1335 (m), 1310 (s), 1290 (s), 1270 (w), 1250 (w), 1240 (w), 1230 (w), 1200 (w), 1160 (m), 1100 (m), 1055 (s), 1045 (s), 1030 (s), 1000 (s), 985 (w), 970 (w), 960 (m), 940 (m), 895 (s), ca. 835 (vs, br, PF_6^-), 810 (vs), 780

(s), 765 (s), 735 (m), 720 (m), 655 (m), 630 (w), 555 (vs). UV−vis (CH_3CN; λ_{max}, nm (ϵ, M^{-1} cm^{-1})): 255 (10 600), 702 (117), 803 (119). Molar conductivity: 148 Ω^{-1} cm^2 mol^{-1}. EPR (CH_2Cl_2/toluene): $g_{||} = 2.248$, $A_{||} = 133 \times 10^{-4}$ cm^{-1}. Magnetism (solid state, room temperature): $\mu_{eff} = 1.88 \pm 0.05$ μ_B/Cu.

11. [Cu(pmap)F]$_2$(PF$_6$)$_2$ (3c-PF$_6$)$_2$. Complex **1c**-PF_6 (1.07 g, 2.03 mmol) was dissolved in 30 mL of argon-saturated CH_3CN and stirred for 10 min. The yellow solution was then bubbled with dry O_2, resulting in an instantaneous color change to blue-green and formation of a small quantity of green precipitate. After being oxygenated for 15 min, the solution was filtered and layered with diethyl ether (100 mL). Refrigeration of the mixture for several days resulted in the deposition of dark-blue crystalline material with a small quantity of green oil. Recrystallization of the solid from CH_3CN/Et_2O gave large blue tabular crystals that were dried in vacuo (48 h) to yield 0.453 g (41% based on Cu) of the title compound. Anal. Calcd for $(C_{20}H_{22}CuF_7N_4P)_2$: C, 44.00; H, 4.06; N, 10.26; F, 24.36. Found: C, 44.28; H, 4.00; N, 10.50; F, 23.93. IR (Nujol; cm^{-1}): ca. 2900 (vs, C−H), 2250 (w), 2000 (w), 1660 (w), 1600 (vs, C═C), 1570 (s), 1450 (vs), 1380 (s), 1320 (s), 1300 (s), 1270 (m), 1220 (w), 1210 (w), 1165 (s), 1100 (m), 1055 (s), 1030 (s), 1000 (s), 980 (w), 970 (w), 960 (m), 950 (m), 900 (vs), ca. 835 (vs, br, PF_6^-), 765 (vs), 735 (s), 650 (m), 630 (w), 590 (s), 555 (vs). UV−vis (CH_3CN; λ_{max}, nm (ϵ, M^{-1} cm^{-1})): 256 (12200), 637 (105). Molar conductivity: 151 Ω^{-1} cm^2 mol^{-1}. EPR (CH_2Cl_2/toluene): $g_{||} = 2.250$, $A_{||} = 168 \times 10^{-4}$ cm^{-1}. Magnetism (solid state, room temperature): $\mu_{eff} = 1.90 \pm 0.05$ μ_B/Cu.

Results and Discussion

Syntheses of Ligands. The syntheses of all four ligands are straightforward and gram amounts of these materials were easily obtained. With the exception of tmpa, which is a white solid, the other three amines pmea, pmap, and tepa are obtained as viscous yellow-to-brown oils. In the course of another study on the thermodynamic behavior of tripodal ligands,[47,48] we obtained crystals of the hydroperchlorate salt of tepa (H(tepa)-ClO_4). An ORTEP plot of its molecular structure is shown in Figure S1 (see Supporting Information for complete listings of crystallographic data). It is interesting to note that crystal structures of protonated tmpa were reported earlier, but here three acidic protons reside on the pyridyl nitrogens, none being located on the amine nitrogen.[49−51] This is different in H(tepa)-ClO_4 in which the amine nitrogen is the most basic and, therefore, protonated first in contrast to tmpa; the proton could be located and refined on the amine nitrogen in the crystal structure.

In contrast to the extensive use of tmpa in bioinorganic chemistry, only a small number of structurally characterized complexes with one of the other three amines as ligand were reported so far (pmea,[45] pmap,[46,52] and tepa[31,53−58]). Here we report the syntheses and characterization of the copper(I)/(II) complexes of these ligands.

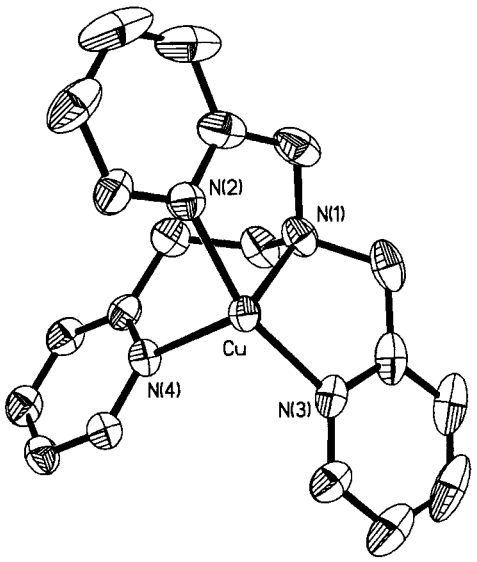

Figure 2. ORTEP plot of the cation of [Cu(pmea)]PF_6 (**1b**-PF_6). The thermal ellipsoids are at the 50% probability level, and the hydrogen atoms are omitted for clarity.

Syntheses and Characterization of Copper(I) Complexes. The monomeric copper(I) complexes $[Cu(tmpa)CH_3CN]^+$ (**1a**), $[Cu(pmea)]^+$ (**1b**), $[Cu(pmap)]^+$ (**1c**), and $[Cu(tepa)]^+$ (**1d**) were prepared in good yield by addition of 1 equiv of $[Cu(CH_3CN)_4]Y$ ($Y = PF_6^-$ or ClO_4^-) to the appropriate ligand in acetonitrile under argon. In the case of tmpa only the copper complex **1a** crystallizes with an additional acetonitrile as ligand. Oxygen-free solutions of **1a**, **1b**, and **1c** are stable in nitrile solvents; however, they are very air-sensitive, decomposing to give green- or blue-colored Cu(II) products upon exposure to O_2 (see below).

The crystal structures of **1a**-ClO_4 as well as of the very similar derivative [Cu(tmpa′)(CH_3CN)]PF_6 (tmpa′ = bis(2-pyridylmethyl)(5-carbomethoxy-2-pyridylmethyl)amine) were reported earlier, and the geometries are described as trigonal bipyramidal.[24,59] Interestingly when triphenylphosphine was used for the stabilization of the $[Cu(I)tmpa]^+$ unit, the crystal structure confirmed the coordination of PPh_3 and showed a tetracoordinate copper(I) ion with a "dangling" uncoordinated pyridyl arm from the ligand.[24]

Structure of [Cu(pmea)]PF$_6$ (1b-PF$_6$). An ORTEP plot of the cationic portion of **1b**-PF_6 is presented in Figure 2. Selected crystallographic data, bond distances, and bond angles are listed in Tables 1 and 2 (see Supporting Information for complete listings).

The structure is four-coordinate, with ligation to the three pyridyl and single aliphatic amine nitrogens of the unsymmetric pmea ligand. The geometry about the copper atom is best described as pyramidal with the amine nitrogen occupying the axial position and the pyridyl nitrogens (N(2), N(3), N(4)) in the trigonal plane. The Cu(I) ion is displaced only 0.028 Å out of the N(2)−N(3)−N(4) plane. The $Cu-N_{amine}$ bond length of 2.158(17) Å in **1b**-PF_6 is much shorter than that of **1a**-PF_6. Equatorial values ($Cu-N_{pyridine}$) are in the range 1.933(12)−2.039(13) Å and therefore slightly shorter than in **1a**-PF_6.

Structure of [Cu(pmap)]PF$_6$ (1c-PF$_6$). An ORTEP plot of the cationic portion of **1c**-PF_6 is presented in Figure 3. Selected

(47) Dittler-Klingemann, A. M.; Orvig, C.; Hahn, F. E.; Thaler, F.; Hubbard, C.; van Eldik, R.; Schindler, S.; Fábián, I. *Inorg. Chem.* **1996**, *35*, 7798−7803.
(48) Thaler, F.; Hubbard, C. D.; Heinemann, F. W.; van Eldik, R.; Schindler, S.; Fabian, I.; Dittler-Klingemann, A. M.; Hahn, F. E.; Orvig, C. *Inorg. Chem.* **1998**, *37*, 4022−4029.
(49) Anderegg, G.; Wenk, F. *Helv. Chim. Acta* **1967**, *30*, 2330−2332.
(50) Britton, D.; Norman, R. E.; Que, L., Jr. *Acta Crystallogr., Sect. C* **1991**, *47*, 2415.
(51) Hazell, A.; McBinley, J.; Toftlund, H. *J. Chem. Soc., Dalton Trans.* **1999**, 1271−1276.
(52) Schindler, S.; Walter, O.; Pedersen, J. Z.; Toftlund, H. *Inorg. Chim. Acta* **2000**, *303*, 215−219.
(53) Karlin, K. D.; Dahlstrom, P. L.; Hayes, J. C.; Simon, R. A.; Zubieta, J. *Cryst. Struct. Commun.* **1982**, *11*, 907−912.
(54) Che, C.; Yam, V. W.-W.; Mak, T. C. W. *J. Am.Chem. Soc.* **1990**, *112*, 2284.
(55) Jiang, F.; Conry, R. R.; Bubacco, L.; Tyeklar, Z.; Jacobson, R. R.; Karlin, K. D.; Peisach, J. *J. Am. Chem. Soc.* **1993**, *115*, 2093−2102.
(56) Baxter, K. E.; Hanton, L. R.; Simpson, J.; Vincent, B. R.; Blackman, A. G. *Inorg. Chem.* **1995**, *34*, 2795−2796.
(57) Xu, X.; Allen, C. S.; Chuang, C.-L.; Canary, J. W. *Acta Crystallogr., Sect. C* **1998**, *54*, 600−601.
(58) Alilou, E. H.; Hallaoui, A. E.; Ghadraoui, E. H. E.; Giorgi, M.; Pierrot, M.; Réglier, M. *Acta Crystallogr., Sect. C* **1997**, *53*, 559−562.
(59) Lim, B. S.; Holm, R. H. *Inorg. Chem.* **1998**, *37*, 4898−4908.

Table 1. Crystal Data and Structure Refinement

	[Cu(I)(pmea)]PF_6 (**1b**-PF_6)	[Cu(I)(pmap)]PF_6 (**1c**-PF_6)	[Cu(II)(pmea)Cl]ClO_4·H_2O (**2b**-ClO_4)·H_2O	[Cu(II)(pmap)Cl]ClO_4 (**2c**-ClO_4)
chemical formula	$C_{19}H_{20}CuF_6N_4P$	$C_{20}H_{22}CuF_6N_4P$	$C_{19}H_{22}Cl_2CuN_4O_5$	$C_{20}H_{22}Cl_2CuN_4O_4$
fw	507.89	526.93	520.85	516.86
temp (K)	294(2)	293(2)	173(2)	293(2)
wavelength (Å)	0.710 73	0.710 73	0.710 73	0.710 73
space group	*Pbca*	*Pbca*	$P\bar{1}$	$P2_1/c$
a (Å)	14.413(3)	13.306(3)	11.967(2)	8.7682(4)
b (Å)	16.043(3)	16.936(3)	12.445(3)	18.4968(10)
c (Å)	18.288(4)	19.163(4)	15.668(3)	13.2575(8)
α (deg)	90	90	84.65(3)	90
β (deg)	90	90	68.57(3)	94.219(4)
γ (deg)	90	90	87.33(3)	90
vol ($Å^3$)	4228(2)	4318(2)	2162.4(7)	2144.3(2)
Z	8	8	4	4
density calcd (Mg/m^3)	1.611	1.621	1.600	1.601
abs coeff (mm^{-1})	1.173	1.153	1.297	1.304
R indices[a] [$I > 2\sigma(I)$]	$R(F_o) = 0.0656$ $R_w(F_o) = 0.0677$	$R1(F_o) = 0.0759$ $wR2(F_o^2) = 0.1882$	$R1(F_o) = 0.0423$ $wR2(F_o^2) = 0.1071$	$R1(F_o) = 0.0354$ $wR2(F_o^2) = 0.0785$
R indices[a] (all data)		$R1(F_o) = 0.1881$ $wR2(F_o^2) = 0.2512$	$R1(F_o) = 0.0571$ $wR2(F_o^2) = 0.1182$	$R1(F_o) = 0.0577$ $wR2(F_o^2) = 0.1202$

[a] $R1(F_o) = \sum||F_o| - |F_c||/\sum|F_o|$. $wR2(F_o^2) = (\sum[w(F_o^2 - F_c^2)^2]/\sum[w(F_o^2)^2])^{1/2}$. $R(F_o) = \sum(|F_o - F_c|)/\sum(F_o)$. $R_w(F_o) = \sum[(|F_o - F_c|)w^{1/2}]/\sum[F_o w^{1/2}]$.

Table 2. Bond Lengths [Å] and Angles [deg] for **1b**-PF_6, **1c**-PF_6, **2b**-ClO_4·H_2O, and **2c**-ClO_4

Bond Lengths for **1b**-PF_6

Cu(1)−N(1)	2.158(17)	Cu(1)−N(3)	1.933(12)
Cu(1)−N(2)	2.039(13)	Cu(1)−N(4)	1.961(14)

Bond Angles for **1b**-PF_6

N(1)−Cu(1)−N(2)	85.6(6)	N(1)−Cu(1)−N(3)	83.3(5)
N(2)−Cu(1)−N(3)	124.9(5)	N(1)−Cu(1)−N(4)	98.9(6))
N(2)−Cu(1)−N(4)	101.6(5)	N(3)−Cu(1)−N(4)	133.4(5)

Bond Lengths for **1c**-PF_6

Cu(1)−N(82)	1.959(6)	Cu(1)−N(52)	2.038(7)
Cu(1)−N(22)	2.009(7)	Cu(1)−N(1)	2.144(6)

Bond Angles for **1c**-PF_6

N(82)−Cu(1)−N(22)	138.4(3)	N(82)−Cu(1)−N(1)	101.6(3)
N(82)−Cu(1)−N(52)	115.6(3)	N(22)−Cu(1)−N (1)	83.2(3)
N(22)−Cu(1)−N(52)	103.8(3)	N(52)−Cu(1)−N(1)	100.6(3)

Bond Lengths for **2b**-ClO_4·H_2O

Cu(1)−N(10)	1.990(3)	Cu(2)−N(60)	2.010(3)
Cu(1)−N(28)	1.990(3)	Cu(2)−N(50)	2.011(3)
Cu(1)−N(47)	2.059(3)	Cu(2)−N(78)	2.050(3)
Cu(1)−N(40)	2.261(3)	Cu(2)−N(70)	2.288(3)
Cu(1)−Cl(1)	2.2742(11)	Cu(2)−Cl(2)	2.2810(11)

Bond Angles for **2b**-ClO_4·H_2O

N(10)−Cu(1)−N(28)	162.16(12)	N(60)−Cu(2)−N(50)	162.20(11)
N(10)−Cu(1)−N(47)	82.82(13)	N(60)−Cu(2)−N(78)	82.84(11)
N(28)−Cu(1)−N(47)	83.30(13)	N(50)−Cu(2)−N(78)	82.28(11)
N(10)−Cu(1)−N(40)	94.40(11)	N(60)−Cu(2)−N(70)	91.69(11)
N(28)−Cu(1)−N(40)	97.70(11)	N(50)−Cu(2)−N(70)	99.05(12)
N(47)−Cu(1)−N(40)	93.98(11)	N(78)−Cu(2)−N(70)	94.06(11)
N(10)−Cu(1)−Cl(1)	95.49(10)	N(60)−Cu(2)−Cl(2)	96.77(9)
N(28)−Cu(1)−Cl(1)	96.10(10)	N(50)−Cu(2)−Cl(2)	96.36(9)
N(47)−Cu(1)−Cl(1)	169.42(8)	N(78)−Cu(2)−Cl(2)	170.82(8)
N(40)−Cu(1)−Cl(1)	96.56(8)	N(70)−Cu(2)−Cl(2)	95.12(8)

Bond Lengths for **2c**-ClO_4

Cu(1)−N(82)	2.015(4)	Cu(1)−N(32)	2.261(4)
Cu(1)−N(62)	2.017(4)	Cu(1)−Cl(1)	2.2690(12)
Cu(1)−N(1)	2.102(3)		

Bond Angles for **2c**-ClO_4

N(82)−Cu(1)−N(62)	169.0(2)	N(1)−Cu(1)−N(32)	93.2(2)
N(82)−Cu(1)−N(1)	81.54(14)	N(82)−Cu(1)−Cl(1)	92.50(10)
N(62)−Cu(1)−N(1)	91.64(14)	N(62)−Cu(1)−Cl(1)	91.86(11)
N(82)−Cu(1)−N(32)	96.7(2)	N(1)−Cu(1)−Cl(1)	164.23(11)
N(62)−Cu(1)−N(32)	92.2(2)	N(32)−Cu(1)−Cl(1)	102.01(10)
N(82)−Cu(1)−N(62)	169.0(2)	N(1)−Cu(1)−N(32)	93.2(2)

crystallographic data, bond distances, and bond angles are listed in Tables 1 and 2 (see Supporting Information for complete listings). The copper(I) ion is tetracoordinate in the solid state, with ligation to the three pyridyl and one aliphatic amine nitrogen donors of the ligand. The $Cu-N_{py}$ bond lengths (1.959(6)−2.038(7) Å) and the copper−amine nitrogen bond ($Cu-N_{amine}$ = 2.144(6) Å) are similar to those found in **1b**-PF_6. The coordination geometry is distorted toward trigonal pyramidal with the pyridyl nitrogens (N(82), N(22), N(52)) in the basal plane and the amine nitrogen (N(1)) occupying the axial position. The presence of a single methylene bridge between the aliphatic amine nitrogen (N(1)) and the pyridine ring containing N(22) provides the source of distortion, producing a strained five-membered chelate ring system that cannot approach the idealized tetrahedral value for the N(1)−Cu(1)−N(22) angle (=83.2(3)°). This has the effect of displacing the Cu(I) ion 0.168 Å above the N(82)−N(22)−N(52) plane in order to accommodate its coordination requirements.

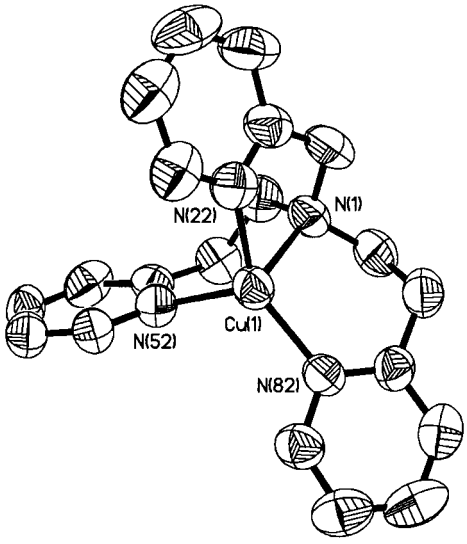

Figure 3. ORTEP plot of the cation of [Cu(pmap)]PF_6 (**1c**-PF_6). The thermal ellipsoids are at the 50% probability level, and the hydrogen atoms are omitted for clarity.

The crystal structure of **1d**-BPh_4 was reported earlier, and the coordination geometry can be described as pseudotetrahedral distorted toward pyramidal with the Cu(I) ion 0.31 Å above the N(2)−N(3)−N(4) plane.[37] The $Cu-N_{amine}$ bond length of 2.192(6) Å in **1d**-BPh_4 is slightly longer than those in **1b**-PF_6

and **1c**-PF_6 but shorter than in **1a**-PF_6. Equatorial values ($Cu-N_{pyridine}$) are in the range 2.012(5)−2.022(5) Å.

X-ray crystal structures of several Cu(I) complexes containing tripodal tetradentate ligands with thioether and nitrogen donors have been described, and a recent summary of references is given by Rorabacher and co-workers.[60] By comparison of the structures of **1a**−**1d** with these other well-characterized systems, a more complete understanding of the influence that the ligand and its donor groups have on the cuprous coordination properties may be realized. Many of these ligands have three identical pendant donor atoms, but a number of tripodal ligand systems have also been reported in which the donor atoms are not identical on all three arms.[60] The length of the hydrocarbon "arms" of the ligands are varied such that they contain either two- or three-atom bridges between ligating termini.

Most of the Cu(I) complexes with these ligands share the common structural feature in that they are all tetracoordinate with molecular geometries, which are distorted from tetrahedral toward pyramidal. The Cu atom is displaced from an ideal tetrahedral position toward the basal plane defined by the donor atoms of the arms of the tripod with the tertiary amine nitrogen occupying the apical position. The degree of distortion from tetrahedral geometry appears to be primarily a function of chelate ring size, with donor type playing a secondary role.

The effect of chelate ring size or ligand "bite" on the molecular geometry of the Cu(I) compounds is clearly evident upon examining the structural parameters of complexes containing three pyridine donors. The data for this series of complexes indicate that reducing the length of the arms of the tripod ligand results in displacement of the Cu(I) ion toward the trigonal plane formed by the pyridine nitrogens. The net effect is distortion of the structure toward pyramidal geometry as a consequence of forming five-membered chelate rings.

It is perhaps somewhat surprising that although in **1a** an additional acetonitrile molecule is coordinated to the copper(I) ion, the crystals of **1b**-PF_6 and **1c**-PF_6 grown from a CH_3CN/Et_2O solvent system show no coordination of an acetonitrile ligand. Here the tmpa ligand in **1a** seems to play a special role that is reflected in solution as well. ^1H and ^{13}C NMR spectra obtained at room temperature for complexes **1a**−**1d** reveal an interesting feature: while **1a** shows broadened signals, **1b**−**1d** ^1H NMR resonances are sharp and appear normal (see Experimental Section).[24,61] The observation of broadened signals is unusual because complexes of the diamagnetic Cu(I) ion (d^{10} system) are generally found to display sharp peaks in their NMR spectra. The broadened signal in **1a** is observed to sharpen as the temperature is decreased from room temperature to −50 °C. At room temperature, the broadened resonances of **1a** are thought to arise because of exchange processes that occur between the pyridyl arms. This exchange conceivably involves the dissociation and reassociation of the pyridyl donors about the cuprous ion, along with probable solvent interactions.

Reaction of Copper(I) Complexes with Dioxygen. The four copper(I) complexes show different reactivity toward dioxygen. The reaction of **1a** with dioxygen was investigated earlier.[23,24] Detailed kinetic studies showed that **1a** reacts reversibly with dioxygen, forming the superoxo complex $[(tmpa)Cu(O_2)]^+$ (λ_{max} = 410 nm (ϵ = 4000 cm^{-1} M^{-1}), 747 nm (ϵ = 1000 cm^{-1} M^{-1})) as a transient intermediate on the way to the ultimate purple μ-peroxo product $[\{Cu(tmpa)\}_2(O_2)]^{2+}$ (λ_{max} = 525 nm (ϵ = 11 500 cm^{-1} M^{-1}), 590 nm (ϵ = 7600 cm^{-1} M^{-1})) according to Scheme 1.[26,28] Thermally and hydrolytically unstable crystals of $[\{Cu(tmpa)\}_2(O_2)]^{2+}$ were obtained at −85 °C, and X-ray data were obtained at −90 °C.[23,24]

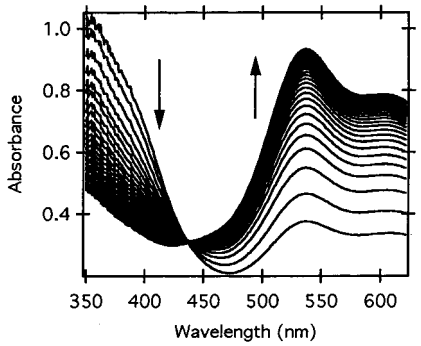

Figure 4. Reaction of **1b** with dioxygen at −90.0 °C in dry propionitrile ([complex] = 0.4 mM, $[O_2]$ = 4.4 mM, Δt = 0.013 s, total time is 0.33 s).

Scheme 1

$$[(L)Cu(RCN)]^+ + O_2 \rightleftharpoons [(L)Cu(O_2)]^+ + RCN$$

$$[(L)Cu(RCN)]^+ + [(L)Cu(O_2)]^+ \rightleftharpoons [(L)Cu(O_2)Cu(L)]^{2+} + RCN$$

$$[(L)Cu(O_2)Cu(L)]^{2+} \rightarrow \text{irreversible decay}$$

When **1b** was reacted with dioxygen in propionitrile at −90 °C, the very fast formation of a purple species was observed. Time-resolved spectra of this reaction are shown in Figure 4.

The spectrum of the product is very similar to that obtained from **1a** under identical conditions; presumably the copper peroxo complex $[\{Cu(pmea)\}_2(O_2)]^{2+}$ (λ_{max} = 536 nm ($\epsilon \approx$ 5000 cm^{-1} M^{-1})) was formed. But this compound starts to decompose rapidly immediately after its formation (this explains the lower ϵ value compared with that of $[\{Cu(tmpa)\}_2(O_2)]^{2+}$), and no further characterization of this complex was possible. Furthermore, in contrast to **1a** the formation of a superoxo complex during the reaction of **1b** with dioxygen was not observed. This is similar to the complex $[(BPQA)Cu]^+$ (BPQA = bis(2-pyridylmethyl)(2-quinolylmethyl)amine).[26] The formation of $[\{Cu(pmea)\}_2(O_2)]^{2+}$ is much faster than the formation of $[\{Cu(tmpa)\}_2(O_2)]^{2+}$ under identical conditions and can be described by a single reaction step with an apparent third-order rate constant. Unfortunately, no exact data fit was possible because of the lability of the complex. Using acetone instead of propionitrile as a solvent had shown a dramatic effect on the reaction of dioxygen with **1a** and similar complexes.[27,62] This was not the case for the reaction of **1b** with dioxygen, indicating that here the competition of a nitrile ligand with dioxygen does not play a major role in solution.

When **1c** was reacted with dioxygen at −90 °C in propionitrile or acetone, no superoxo or peroxo intermediate could be detected spectroscopically using stopped-flow techniques. In contrast to complexes **1a**−**1c**, complex **1d** is completely unreactive toward dioxygen; solutions of this complex remain yellow even after prolonged treatment with dioxygen.

Syntheses and Characterization of Copper(II) Complexes. As described earlier, reaction of **1a**-PF_6 with O_2 at room temperature resulted in the formation of a mixture of the

(60) Ambundo, E. A.; Deydier, M.-V.; Grall, A. J.; Aguera-Vega, N.; Dressel, L. T.; Cooper, T. H.; Heeg, M. J.; Ochrymowycz, L. A.; Rorabacher, D. B. *Inorg. Chem.* **1999**, *38*, 4233−4242.

(61) Jacobsen, R. R. Synthesis, characterization and reactivity of copper(I) and copper(II) complexes containing tripodal tetradentate ligands. Ph.D. Thesis, State University of New York at Albany, Albany, NY, 1989.

(62) Becker, M.; Heinemann, F.; Schindler, S. *Chem.*−*Eur. J.* **1999**, *5*, 3124−3129.

dinuclear fluoride-bridged complex $[Cu(tmpa)F]_2(PF_6)_2$ (**3a**-PF_6) and the mononuclear complex $[Cu(tmpa)F](PF_6)\cdot CH_2Cl_2$, both characterized by X-ray crystallography.[63]

1. Copper(II) Fluoride Complex of pmea and pmap. The fluoride complexes $[Cu(pmea)F]_2(PF_6)_2$ (**3b**-PF_6) and $[Cu(pmap)F]_2(PF_6)_2$ (**3c**-PF_6) were prepared by the decomposition reactions of **1b**-PF_6 and **1c**-PF_6, respectively, with molecular oxygen in acetonitrile solution (ambient temperature). No equivalent fluoride complex could be obtained from **1d**-PF_6 because of the unreactivity of this complex toward dioxygen. Presumably, decomposition of the PF_6^- anion occurs during reaction of the Cu(I) complex with O_2, releasing the F^- ion that can then be incorporated into the cupric compounds.

In contrast to the crystals of **3c**-PF_6, crystals of **3b**-PF_6 were suitable for X-ray structural analysis. As with **3a**-PF_6, **3b**-PF_6 is a dimeric compound that is centrosymmetric, and an ORTEP plot of one copper cation of **3b**-PF_6 is shown in Figure S2a (see Supporting Information for complete listings of crystallographic data). The structure consists of a pentacoordinate Cu(II) ion with ligation to the tetradentate pmea ligand and single fluoride ion in a distorted square pyramidal arrangement. The axial position in **3b**-PF_6 is occupied by the nitrogen atom of the pyridine ring that is bonded to the long arm of the pmea ligand (N(4)); the basal sites are occupied by the remaining pyridyl (N(2), N(3)) and aliphatic amine (N(1)) nitrogens and the fluoride ion (F1). The Cu atom is displaced 0.123 Å out of the basal plane in a direction toward the axial pyridyl group. Equatorial $Cu-N_{py}$ distances are Cu(1)−N(2) = 1.983(7) Å and Cu(1)−N(3) = 1.993(7) Å, while the axial $Cu-N_{py}$ bond length is somewhat longer at 2.334(7) Å. The remaining equatorial bond lengths are Cu−F = 2.047(4) Å and $Cu-N_{amine}$ = 2.033(7) Å.

As mentioned above, the full structure of **3b**-PF_6 is dimeric (Figure S2b of Supporting Information), consisting of two monomeric $[Cu(pmea)F]^+$ units bridged by long Cu−F interactions; the Cu···Cu distance is 3.539(1) Å, which is considerably longer than that reported for other fluoro-bridged Cu(II) dimers.[64−66] The extremely long Cu−F bond length (2.870(6) Å) indicates that the interaction between the two monomeric units is weak, possibly resulting from solid-state effects such as crystal packing; in solution the monomers probably dissociate from one another (vide infra).

Comparison of the structural parameters for **3b** and **3a** reveals that the two compounds have similar coordination environments about Cu(II). The main differences lie in the Cu−F bond distance (1.862(4) Å in **3a** compared to 2.047(4) Å in **3b**) and the location of the axial pyridine ligand.

2. Copper(II) Chloride Complexes. The four copper(II)−chloride complexes $[Cu(tmpa)Cl]^+$ (**2a**), $[Cu(pmea)Cl]^+$ (**2b**), $[Cu(pmap)Cl]^+$ (**2c**), and $[Cu(tepa)Cl]^+$ (**2d**) were easily prepared by the reaction of the cupric salts with the tripodal ligands. Crystal structures of complexes **2a** and **2d** were reported earlier.[31] These two compounds exhibit markedly different structural behavior. Complex **2d** has a distorted square pyramidal coordination geometry with one of the pyridines in the axial position. In contrast, the structure of **2a** is very close to trigonal bipyramidal.

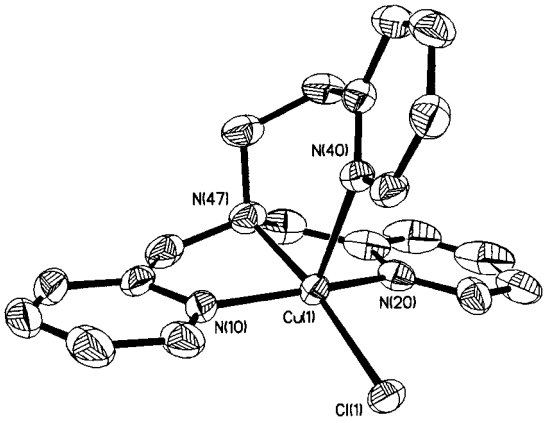

Figure 5. ORTEP plot of the cation of $[Cu(pmea)Cl]ClO_4\cdot H_2O$ (**2b**-ClO_4)·H_2O. The thermal ellipsoids are at the 50% probability level, and the hydrogen atoms are omitted for clarity.

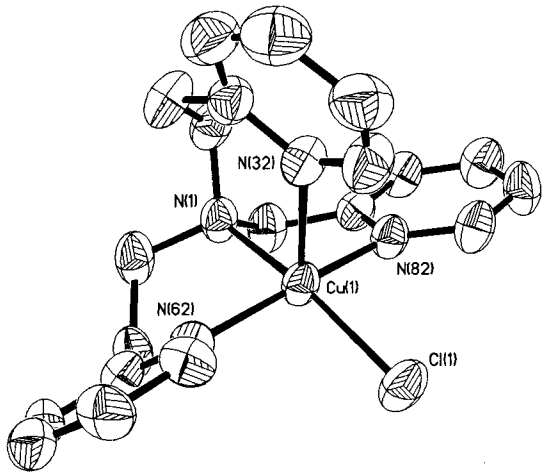

Figure 6. ORTEP plot of the cation of $[Cu(pmap)Cl]ClO_4$ (**2c**-ClO_4). The thermal ellipsoids are at the 50% probability level, and the hydrogen atoms are omitted for clarity.

The structure of **2b**-$ClO_4\cdot H_2O$ contains two crystallographically independent cations (with slightly different bond lengths and angles) in the asymmetric unit. They differ in regard to the orientation of the CH_2-CH_2 arm of the pyridine; in one cation this arm is pointing to the right side, while in the other it points to the left. Only one of two cations is shown in the ORTEP plot in Figure 5. Selected crystallographic data, bond distances, and bond angles are listed in Tables 1 and 2 (see Supporting Information for complete listings).

An ORTEP drawing of the cationic portion of **2c**-ClO_4 is shown in Figure 6. Selected crystallographic data, bond distances, and bond angles are listed in Tables 1 and 2 (see Supporting Information for complete listings).

Some problems occurred during our efforts to obtain crystals of **2b** and **2c** suitable for crystallographic characterization. This was a consequence of these complexes having a tendency to include solvent molecules into the crystal lattice. Complex **2b** crystallized with a different number of water molecules according to the elemental analysis of crystals, showing a lighter or darker blue color. Crystals of **2b** used for structural characterization had one molecule of water in the complex. Depending on the conditions for crystallizing **2c**, it was possible to obtain it without a solvent molecule (Figure 6), with some dichloromethane (see Experimental Section), or with one water molecule. In the last case it turned out that the water molecule is very close to the coordinated chloride ion (Cl(1)···O(100) 3.123(5) Å). Most likely this is a consequence of weak hydrogen

(63) Jacobson, R. R.; Tyeklár, Z.; Karlin, K. D.; Zubieta, J. *Inorg. Chem.* **1991**, *30*, 2035−2040.
(64) Reedijk, J. *Comments Inorg. Chem.* **1982**, *1*, 379−389.
(65) van Rijn, J.; Reedijk, J.; Dartmann, M.; Krebs, B. *J. Chem. Soc., Dalton Trans.* **1987**, 2579−2593.
(66) Keji, F. S.; de Graaff, R. A. G.; Haasnoot, J. G.; Oosterling, A. J.; Pedersen, E.; Reedijk, J. *J. Chem. Soc., Chem. Commun.* **1988**, 423−425.

bonding between the water molecule and the chloride ion. An ORTEP drawing of the cationic portion of **2c**-ClO_4·H_2O is shown in Figure S3 (see Supporting Information for complete listings of crystallographic data). As a consequence of the additional water molecule in **2c**-ClO_4·H_2O, the cell parameters of this complex are different from those of **2c**-ClO_4 but bond lengths and angles are similar.

All the Cu(II) atoms of **2a**−**2d** are pentacoordinated structures with three pyridyl nitrogens, one amino nitrogen, and a chloride. The coordination geometry has been analyzed by using a procedure developed by Addison et al.[67] In this method, a structural index parameter, τ, is calculated in order to describe a complex geometry. The two possible limiting geometries for a five-coordinate metal center are square pyramidal and trigonal bipyramidal. For a perfect square pyramidal geometry τ is equal to zero, while it becomes unity for a perfect trigonal bipyramidal geometry.

As applied to **2a**, the analysis results indicate that this complex adopts a nearly perfect trigonal bipyramidal structure; the three pyridyl nitrogens comprise the equatorial plane and $\tau = 1.01$.[32] The same was observed for other copper(II) complexes of tmpa where X = CH_3CN, H_2O, O_2, F^-, or CN^- instead of Cl^- in $[Cu(tmpa)X]^{n+}$.[23,59,61,63,68,69] In contrast, the structures of complexes **2b**−**2d** adopt a nearly square-based pyramidal geometry with τ values close to zero. Disturbing the symmetry of the ligand tmpa by modifying the pyridyl arms has the consequence that the copper(II) complexes prefer a square-based pyramidal geometry. This was observed not only for the ligand modification from tmpa to tepa as described here but also for other ligand modifications of tmpa.[32,68]

UV−Vis Spectra of the Copper(II) Complexes. The copper(II) complexes of the tripod ligands are characterized by a rather broad d−d absorption band (ca. 650−1000 nm) in their solution electronic spectra; often, a low- or high-energy shoulder is also present or, occasionally, two distinct absorption maxima are observed. In many cases it has been shown that the presence of a single d−d band with a high-energy shoulder is typical of a trigonal bipyramidal stereochemistry for copper, whereas an absorption with a low-energy shoulder indicates a square pyramidal geometry.[30,31,70−75] Examination of the electronic spectral data of the copper(II) complexes (see Experimental Section) demonstrates that, on the basis of the above criterion, **2d** adopts a square pyramidal geometry in solution while **2a** must be described as trigonal bipyramidal. Complexes **2b** and **2c** have geometries that are distorted slightly from an ideal square pyramidal geometry but do not closely approach a trigonal bipyramidal stereochemistry.

The UV−vis spectrum of the fluoride-bridged complex **3b** in acetonitrile exhibits two bands of nearly equal intensity between 670 and 890 nm and is similar to the spectrum of **3a**. This pattern suggests that the geometry about the copper ion in solution is between square pyramidal and trigonal bipyramidal. For **3b**, a geometry between these two extremes would indicate a reorganization of the coordination sphere because the solid-state structure shows a stereochemistry that is very nearly square pyramidal. Dissociation of the monomeric units in solution could be responsible for this change in structure due to loss of stabilizing intermolecular interactions. Alternatively, the solution spectrum of **3b** may indicate that an equilibrium mixture of the two limiting geometric forms is present or that a monomer−dimer equilibrium exists. The solution spectrum of **3c** clearly indicates a square pyramidal geometry.

Electron Paramagnetic Resonance (EPR), Magnetic, and Conductivity Measurements. It is known that the EPR spectral pattern for square pyramidal complexes of Cu(II) ($d_{x^2-y^2}$ ground state) is quite different from that observed for trigonal bipyramidal coordination (d_{z^2} ground state). In general, frozen solution EPR spectra of tetragonal (SP) complexes are characterized by an axial pattern with the features $g_{\|} > 2.1 > g_{\perp} > 2.0$ and $|A_{\|}| = (120-150) \times 10^{-4}$ cm^{-1}.[71,74,76−80] On the other hand complexes with trigonal bipyramidal coordination typically show EPR spectra having a "reversed axial" appearance with $g_{\perp} > g_{\|} \approx 2.0$ and $|A_{\|}| = (60-100) \times 10^{-4}$ cm^{-1}.[71,76−80] Thus, in general, the coordination geometry around the metal ion in Cu(II) complexes can be deduced from an examination of the EPR spectral features except for those structures that are between square pyramidal and trigonal bipyramidal coordination.

EPR spectra of the present series of cupric complexes have been recorded for frozen solution samples (CH_2Cl_2/toluene), 4:1 v/v) at 77 K (X-band frequency). The complexes of tepa, pmap, and pmea appear to exhibit axial spectra typical of square pyramidal species with $g_{\|}$ varying from 2.207 to 2.250 and $|A_{\|}|$ having a range from 133×10^{-4} to 176×10^{-4} cm^{-1} (see Experimental Section). These results are in general agreement with the solution electronic spectra, which also suggest the existence of square pyramidal geometries. Any minor distortions from this geometry, which may exist in complexes containing pmap or pmea, are not apparent from examination of the EPR spectra, which show only a pattern characteristic of tetragonal coordination. As reported earlier, the EPR spectra of the tmpa complexes $[(tmpa)CuX]^{z+}$ (X = Cl^-, Br^-, N_3^-, Me−Im) all display a reversed axial appearance indicative of trigonal bipyramidal geometry about the Cu(II) ion.[31,61] These compounds display spin Hamiltonian parameters that are expected for this coordination stereochemistry with $|A_{\|}|$ values being low ($< 87 \times 10^{-4}$ cm^{-1}) and $g_{\|} \approx 2.0$. Again, the results obtained are in general agreement with the solution electronic spectra that predict a trigonal bipyramidal stereochemistry for these complexes.

X-band EPR spectra were also recorded for powder samples of the fluoride complexes **3b**-PF_6 and **3c**-PF_6 at room temperature. As expected, a well-resolved spectrum typical of isolated copper dimers[81−83] was obtained for **3b**-PF_6 in accordance with the known solid-state structures. A similar spectral pattern was observed for **3c**-PF_6, indicating the dimeric nature of this

(67) Addison, A. W.; Rao, T. N.; Reedijk, J.; van Rijn, J.; Verschoor, G. C. *J. Chem. Soc., Dalton Trans.* **1984**, 1349−1356.
(68) Nagao, H.; Komeda, N.; Mukaida, M.; Suzuki, M.; Tanaka, K. *Inorg. Chem.* **1996**, *35*, 6809−6815.
(69) Corsi, D. M.; Murthy, N. N.; Young, V. G., Jr.; Karlin, K. D. *Inorg. Chem.* **1999**, *38*, 848−858.
(70) Nakao, Y.; Onoda, M.; Sakurai, T.; Nakahara, A.; Kinoshita, I.; Ooi, S. *Inorg. Chim. Acta* **1988**, *151*, 55−59.
(71) Addison, A. W.; Hendriks, H. M. J.; Reedijk, J.; Thompson, L. K. *Inorg. Chem.* **1981**, *20*, 103−110.
(72) Ciampolini, M.; Nardi, N. *Inorg. Chem.* **1966**, *5*, 41−44.
(73) Albertin, G.; Bordignon, E.; Orio, A. A. *Inorg. Chem.* **1975**, *14*, 1411−1413.
(74) Duggan, M.; Ray, N.; Hathaway, B.; Tomlinson, G.; Briant, P.; Plein, K. *J. Chem. Soc., Dalton Trans.* **1980**, 1342−1348.
(75) Hathaway, B. J.; Billing, D. E. *Coord. Chem. Rev.* **1970**, *5*, 143−207.
(76) Thompson, L. K.; Ramaswamy, B. S.; Seymout, E. A. *Can. J. Chem.* **1977**, *55*, 878.
(77) Nishida, Y.; Oishi, N.; Kida, S. *Inorg. Chim. Acta* **1980**, *44*, L257−L258.
(78) Takahashi, K.; Ogawa, E.; Oishi, N.; Kida, S. *Inorg. Chim. Acta* **1982**, *66*, 97−103.
(79) Barbucci, R.; Bencini, A.; Gatteschi, D. *Inorg. Chem.* **1977**, *16*, 2117−2120.
(80) Morpurgo, L.; Falcioni, R.; Rotildo, G.; Desideri, A.; Mondovi, B. *Inorg. Chim. Acta* **1978**, *28*, L141−L143.

Table 3. Electrochemical Data[a]

compound	$E_{1/2}$ (V)	ΔE (mV)
2a-PF_6	−0.386	140
2b-PF_6	−0.300	100
2c-PF_6	−0.200	200
2d-PF_6	+0.115	230

[a] $E_{1/2} = (E_p^{red} + E_p^{ox})/2$ (vs NHE); $\Delta E = E_p^{red} + E_p^{ox}$; scan rate = 100 mV s^{-1}.

complex, which probably has a structure similar to that of **3b**-PF_6. Also found in these spectra are features corresponding to $\Delta M_s = 2$ transitions at $g \approx 4$, thus confirming the occurrence of Cu···Cu magnetic exchange interactions.

Magnetic moments of the cupric complexes were measured for powder samples at room temperature. As seen from the data (see Experimental Section), all compounds possess moments that are close to the values expected (around 1.7−2 μ_B) for systems without significant Cu(II)−Cu(II) coupling interactions. For the monomeric compounds these results were expected. In the case of the fluoride complexes, however, the results were somewhat surprising because the solid-state structures and the powder EPR spectra clearly indicate the existence of dimeric species capable of coupling interactions. The apparent lack of even moderate coupling between the copper centers, however, can be explained by examining the structures of compounds **3a**-PF_6 and **3b**-PF_6. The coordination geometry about each copper ion is essentially square pyramidal, resulting in a magnetic orbital consisting mainly of $d_{x^2-y^2}$. Because the two magnetic orbitals in each dimer are not in the same plane, overlap between them is minimal and the magnetic interaction is thus small. Similar results were obtained for a copper(II) complex containing bridging hydroxide ligands in a parallel−planar structure; powder EPR spectra indicated a dimeric structure, but room-temperature magnetic susceptibility measurements showed little or no coupling interactions between copper.[84]

Molar conductivities of the complexes were measured in acetonitrile at room temperature, and the values (see Experimental Section) obtained are within the range expected for 1:1 electrolytes.[85] These results indicate that the entire series of compounds exist in solution predominantly as monomeric species without appreciable intermolecular association. This finding is of particular significance in the case of the dimeric fluoride complexes because it indicates that these compounds dissociate substantially or completely in solution.

Electrochemistry. The half-wave potentials of the ligand−cupric chloride complexes **2a**−**2d** were determined by cyclic voltammetry, and the results are summarized in Table 3.[31] In DMF all compounds displayed a quasi-reversible voltammogram having $i_{pc}/i_{pa} \approx 1$ in the range +0.115 to −0.386 V vs NHE with ΔE = 140−230 mV. The influence of ligand flexibility on the electrochemical behavior of these complexes is apparent from these data. Thus, each increase in ligand arm length (i.e., increase in chelate ring size) results in a corresponding increase in redox potential. For example, the difference in redox potential for **2d** vs **2c** is about 0.3 V, resulting in **2d** being stabilized as Cu(I) relative to **2c**. The range of redox potentials measured over the series for the $[(L)Cu(II)Cl]^+$ complexes parallels the range also observed for measurements on the corresponding $[(L)Cu(I)]^+$ compounds as shown for the series $[(tmpa)Cu(I)\text{-}CH_3CN]^+$ through $[(L_Q)Cu(I)]^+$.[29,32]

The redox potential differences observed in these systems have been interpreted as arising from the difference in stability constants for Cu(II)−tripod species.[30,60,86] These studies have shown that Cu(II) favors chelation in a five-membered ring; therefore, compounds containing shorter ligand arms (e.g., tmpa and pmea) are stabilized in higher oxidation states. Thus, conformational constraints imposed by the ligands have substantial effects on the redox properties of copper ion centers in these complexes. A detailed investigation of the influence of coordination geometry on copper(II/I) redox potentials of a series of copper complexes (including **2a** and **2d**) was recently described by Rorabacher and co-workers.[60] The authors report that (i) the nature of the donor atoms, (ii) the number of the donor atoms, (iii) the chelate ring size, and (iv) the general ligand morphology have an almost negligible impact on $K_{Cu(I)L}$ values. By contrast, the stability of the Cu(II)L complexes is drastically affected by all of these parameters. From these findings they conclude that it is largely misleading to state that any specific ligand "stabilizes" the Cu(I) oxidation state to a significant extent.

Summary/Conclusions

The tripod ligands tmpa, pmea, pmap, and tepa readily form copper(I) or copper(II) complexes, a series of compounds for which the structure and physical properties vary systematically as the arm lengths were increased from tmpa to tepa. Additionally, dinuclear fluoride complexes were obtained through the decomposition reactions of **1a**-PF_6, **1b**-PF_6, or **1c**-PF_6 with O_2 in CH_3CN.

Spectroscopic measurements (EPR, UV−vis) were found to be generally consistent with a square pyramidal geometry for the complexes containing tepa, pmap, and pmea ligands. Complexes containing tmpa, on the other hand, were observed to be trigonal bipyramidal. Electrochemical measurements showed a profound effect of the ligand on the Cu(II)/Cu(I) redox couple. Thus, those complexes containing short ligand arms (e.g., pmea, tmpa) were observed to have redox potentials that were more negative than those with longer arms (pmap, tepa). These results indicate that complexes with five-membered chelate rings are stabilized as Cu(II) relative to those with six-membered chelate rings.

Our findings clearly demonstrate the influence of chelate ring size on the stability (or inertness) of copper "dioxygen" complexes. **1a** reacts very quickly with dioxygen to form a superoxo complex that further reacts to form a peroxo complex, which is stable at low temperatures. Only one chelate ring is increased in **1b**, and we find that no superoxo complex could be detected during its reaction with dioxygen; the peroxo complex that formed immediately starts to then undergo further reactions. But here it should be kept in mind that it is not only the chelate ring size that differs between **1a** and the other copper(I) complexes but also the coordination of a nitrile ligand. This ligand is coordinated not only in the solid state but also in solution, and for that reason the reactions of **1a** with dioxygen (and the stability of "dioxygen" complexes) are affected dramatically by the solvent used.[27,62] Therefore, for evaluation of the effect of chelate ring sizes, it is better to compare the

(81) Davis, W. M.; Lippard, S. J. *Inorg. Chem.* **1985**, *24*, 3688−3691.
(82) Bencini, A.; Fabretti, A. C.; Zanchini, C.; Zannini, P. *Inorg. Chem.* **1987**, *26*, 1445−1449.
(83) Drew, M. G. B.; Nelson, S. M.; Reedijk, J. *Inorg. Chim. Acta* **1982**, *64*, L189−L191.
(84) Karlin, K. D.; Gultneh, Y.; Hayes, J. C.; Zubieta, J. *Inorg. Chem.* **1984**, *23*, 519−521.
(85) Geary, W. J. *Coord. Chem. Rev.* **1971**, *7*, 81−122.
(86) Augustin, M. A.; Yandell, J. K.; Addison, A. W.; Karlin, K. D. *Inorg. Chim. Acta* **1981**, *55*, L35−L37.

reactions of **1b** and **1c**. Both complexes are very similar, and no nitrile molecule is coordinated. In contrast to **1b**, where a peroxo analogue forms, the stopped-flow kinetic investigation showed that neither a superoxo nor a peroxo intermediate was observable during the reaction of **1c** with dioxygen. Our data suggest that when tripod ligands are employed, five-membered chelated rings need to be used in order to stabilize long-lived copper−dioxygen adducts. Related to this are the geometric differences in the complexes with varying chelate ring size; the stability of the peroxo ligand in **1a** relative to the stability of a peroxo ligand in **1b** and **1c** might be related to the fact that **1a** has trigonal bipyramidal geometry whereas **1b** and **1c** are found in distorted (toward square pyramidal) structures and therefore are more kinetically labile.[87,88] Tolman and co-workers also have recently seen significant chelate ring size effects on copper−dioxygen chemistry.[88] Further systematic investigations are needed to clarify the coordination geometric factors influencing Cu−(O_2) kinetics of formation, stability, and subsequent reactivity. In contrast, the donor atoms coordinated to the copper ion appear to be less important. For example, some of us recently showed that a copper(I) complex with Me_6tren (=tris(2-dimethylaminoethyl)amine) as ligand also formed a stable copper peroxo complex at low temperatures when reacted with dioxygen.[62]

Acknowledgment. Siegfried Schindler gratefully acknowledges the Deutsche Forschungsgemeinschaft, the Volkswagen-Stiftung, and Prof. Rudi van Eldik for support of this work. K. D. Karlin acknowledges the National Institutes of Health for support of this research.

Supporting Information Available: Complete information on all crystal structure studies and three figures (ORTEP diagrams of H(tepa)-ClO_4, $[Cu(pmea)F]_2(PF_6)_2$ (**3b**-PF_6), and $[Cu(pmap)Cl]ClO_4 \cdot H_2O$ (**1c**-$ClO_4 \cdot H_2O$) are available. This material is available free of charge via the Internet at http://pubs.acs.org. The crystallographic data were deposited as Supplementary Publication Nos. CCDC 145169 to 145173, 147091, and 147768 at the Cambridge Crystallographic Data Center and are available on request from CCDC, 12 Union Road, Cambridge CB21EZ (fax, (+44)1223-336-033; e-mail, deposit@ccdc.cam.ac.uk).

IC000924N

(87) Powell, D. H.; Merbach, A. E.; Fábián, I.; Schindler, S.; van Eldik, R. *Inorg. Chem.* **1994**, *33*, 4468−4473.
(88) Lam, B. M. T.; Jalfen, J. A.; Young, V. G., Jr.; Hagadorn, J. R.; Holland, P. L.; Lledós, A.; Cucurull-Sánchez, L.; Novoa, J. J.; Alvarez, S.; Tolman, W. B. *Inorg. Chem.* **2000**, *39*, 4059−4072.